6th European Conference on Computational Mechanics (ECCM 6)
7th European Conference on Computational Fluid Dynamics (ECFD 7)
1115 June 2018, Glasgow, UK

A ROBUST EXPERIMENT DESIGN FOR THE INVESTIGATION OF NON-IDEAL COMPRESSIBLE-FLUID FLOW EFFECTS

MARTA ZOCCA[1], GIULIO GORI[2⋆], OLIVIER LE MAITRE[3], PIETRO M. CONGEDO[2] and ALBERTO GUARDONE[1]

[1] Department of Aerospace Science & Technology, Politecnico di Milano, Via La Masa 34, 20156 Milano, Italy, martamaria.zocca@polimi.it and alberto.guardone@polimi.it

[2] DeFI Team, CMAP Lab (Ecole Polytechnique, Inria Saclay - Ile de France), 1 rue Estienne d'Orves, 91120 Palaiseau, France, giulio.gori@inria.fr and pietro.congedo@inria.fr

[3] LIMSI, CNRS, Universit Paris-Saclay, Bt 508, rue John von Neumann, Campus Universitaire, F-91405 Orsay, olm@limsi.fr

Key words: Non-ideal Compressible-Fluid Dynamics, NICFD validation, siloxane fluid MDM, Benchmark test case, NICFD verification, ORC applications

Abstract. This paper presents the design process of a converging-diverging nozzle operating with a siloxane MM flow in a highly Non-Ideal regime. In particular, the value of the static pressure and of the Mach number are expected to be measured at selected locations within the nozzle. The goal is to extend the database of experimental results concerning non-ideal compressible-fluid flows. The Method of Characteristics (MOC) is used to design a set of possible nozzle layouts which are suitable for the observation of a non-monotonic Mach number trend throughout a supersonic expansion. To verify that the design satisfies the objectives, a Non-Ideal Computational Fluid Dynamics solver is used to carry out a sensitivity analysis of the Mach number by considering the aleatory uncertainties that necessarily affect the nominal operating conditions. The most robust layout, with respect to the considered uncertainties, is then chosen among a four different configurations. The selected nozzle will be eventually employed within an experimental test rig to collect data regarding Non-Ideal flows.

1 INTRODUCTION

Non-ideal compressible fluid dynamics (NICFD) is devoted to the investigation of the thermo-physical properties of fluid flows whose behavior do not abide by the Polytropic Ideal Gas gas law $Pv = RT$. Departure from ideal behavior is typically observed in fluids made of complex molecules, operating in thermodynamic conditions close to the liquid-vapour saturation curve and critical point. A thorough understanding of NICFD is relevant to both fundamental research in the field of fluid mechanics and to industrial applications. In this respect, understanding NICFD flow phenomena is essential for the

design and operation of *Organic Rankine Cycle* (ORC) plants, namely Rankine cycles using molecularly-complex organic compounds instead of water as working fluid (see e.g. Ref. [1] for a comprehensive review).

Currently, the amount of experimental data related to Non-Ideal Compressible-Fluid flows is quite limited [10] and so is our understanding of the related physical phenomena. Unfortunately, the reliability of Computational Fluid Dynamics (CFD) solvers remains highly questionable, since the lack of experimental data amplifies the uncertainty of the physical models embedded in the numerical tools (i.e. the thermodynamic equations of state and turbulence models).

The goal of the present work is to perform a robust design of a novel experiment aimed at the observation a non-monotone Mach number profile along the supersonic expansion of siloxane MM (Hexamethyldisiloxane, $C_6H_{18}OSi_2$) in a de Laval nozzle. The envisaged experiment will be run in the TROVA blow-down wind tunnel of Politecnico di Milano [12] to provide evidence to this peculiar non-ideal behaviour predicted by the NICFD theory and by computational tools implementing state-of-the-art thermodynamic models. The acquired experimental data will then extend the existing experimental database for NICFD flows.

The present paper is structured as follows. In Sec. 2, test conditions are defined and a set of different nozzles are designed using the Method of Chracteristics (MoC) and state-of-the-art thermodynamic models [6]. Section 3 introduces the Uncertainty Quantification (UQ) framework and the techniques used to assess the robustness of the design. Eventually, in Sec. 4, the results of the sensitivity analysis are reported. In Sec. 5, final comments are provided.

2 EXPERIMENT DESIGN

A brief overview of the experimental set-up and measurement techniques implemented in the TROVA facility is given in Sec. 2.1. The test conditions and the possible geometrical configurations of the test section are then presented and discussed in Sec. 2.2 and Sec. 2.3.

2.1 Experimental facility

The TROVA is a supersonic blow-down wind tunnel designed to investigate NICFD flows of a wide variety of organic fluids. The fluid is supplied by a high-pressure storage tank, the High Pressure Vessel (HPV), and it is discharged in a converging-diverging nozzle providing a supersonic flow. Specifically, the wind-tunnel nozzle is made of contoured profiles, which can be easily replaced whenever a different geometry has to be tested. The test section has a planar configuration, which facilitates the implementation of optical diagnostic techniques, such as schlieren visualizations and Laser Doppler Velocimetry.

For the experiments designed in the present work, the working fluid is the siloxane compound MM and the wind-tunnel test section to be designed consists of a planar converging-diverging nozzle. The reservoir pressure and temperature are measured in the settling chamber upstream of the test section, while static pressure measurements are performed at selected locations along the nozzle axis, to acquire the expansion profile.

Pressure transducers have a full scale in the range 3.5-40 bar. Their expanded uncertainty is 0.07% of the full scale (95% confidence interval). The total temperature in the settling chamber is measured using a thermocouple: the calibration process results in expanded uncertainties of 1.2 ℃.

Schlieren visualizations are exploited to directly measure the Mach number from the slope of the observed Mach waves, as described in Ref. [10]. The measurement is expressed with an expanded uncertainty (Gaussian, 95% confidence level) $U_M = M\sqrt{M^2-1}\,U_\mu$, where M is the Mach number and U_μ is the angular expanded uncertainty (95% confidence level). The uncertainty of the Mach number measurements U_M increases with the Mach number since the well known relation $M = \sin(1/\mu)$ applies. Further details regarding the TROVA test rig and the measurement techniques implemented can be found in Ref. [12, 6, 11].

2.2 Supersonic nozzle flows featuring a supersonic Mach trend

The dynamic behaviour of non-ideal compressible-fluid flows in converging-diverging nozzles qualitatively and quantitatively depends on the so-called *fundamental derivative of gasdynamics* Γ, defined in Ref. [13] as:

$$\Gamma = 1 + \frac{c}{v}\left(\frac{\partial c}{\partial P}\right)_s \tag{1}$$

where c is the speed of sound, v is the specific volume, P is the pressure, and s is the specific entropy per unit mass. For ideal gases, Γ is always > 1, regardless of their thermodynamic state. Conversely, molecularly complex fluids having sufficiently large specific heats are prone to exhibiting $\Gamma < 1$ in the neighborhood of the saturated vapor line, at pressures and temperatures of the order of the critical values. In the present work, steady isentropic expansions in supersonic nozzles operating in the $0 < \Gamma < 1$ regime, called *non-ideal classical regime*, are studied. Under the quasi-one-dimensional assumption, the model for steady isentropic nozzle flows (see e.g. Ref. [14]), the flow Mach number M can be expressed as function of the density ρ only, with the specific entropy per unit mass $\bar{s}$ and the specific total enthalpy per unit mass $\bar{h}^t$ acting as constant parameters. Entropy is indeed constant by assumption, while the condition of constant total enthalpy is enforced by the energy conservation law. The function $M(\rho;\bar{s},\bar{h}^t)$ reads:

$$M(\rho;\bar{s},\bar{h}^t) = \frac{u(\rho;\bar{s},\bar{h}^t)}{c(\bar{s},\rho)} = \frac{\sqrt{2\left[\bar{h}^t - h(\bar{s},\rho)\right]}}{c(\bar{s},\rho)} \tag{2}$$

where u is the streamwise component of the flow velocity and h the specific enthalpy per unit mass. Derivation of the above relation with respect to density yields:

$$\frac{\mathrm{d}M}{\mathrm{d}\rho}(\rho;\bar{s},\bar{h}^t) = \frac{M(\rho;\bar{s},\bar{h}^t)}{\rho} J(\rho;\bar{s},\bar{h}^t) \tag{3}$$

where the function $J(\rho;\bar{s},\bar{h}^t)$ is defined as:

$$J(\rho;\bar{s},\bar{h}^t) = 1 - \Gamma(\bar{s},\rho) - \frac{1}{M^2(\rho;\bar{s},\bar{h}^t)} \tag{4}$$

	Reservoir conditions		Exhaust conditions	
	P^t/P_c	T^t/T_c	P_e/P_c	M_e
Process 1	1.495	1.078	0.248	1.7
Process 2	1.547	1.082	0.255	1.7
Process 3	1.598	1.085	0.259	1.7

Table 1: Processes. Table reports the characterization of the expansion processes considered for the design of the nozzles.

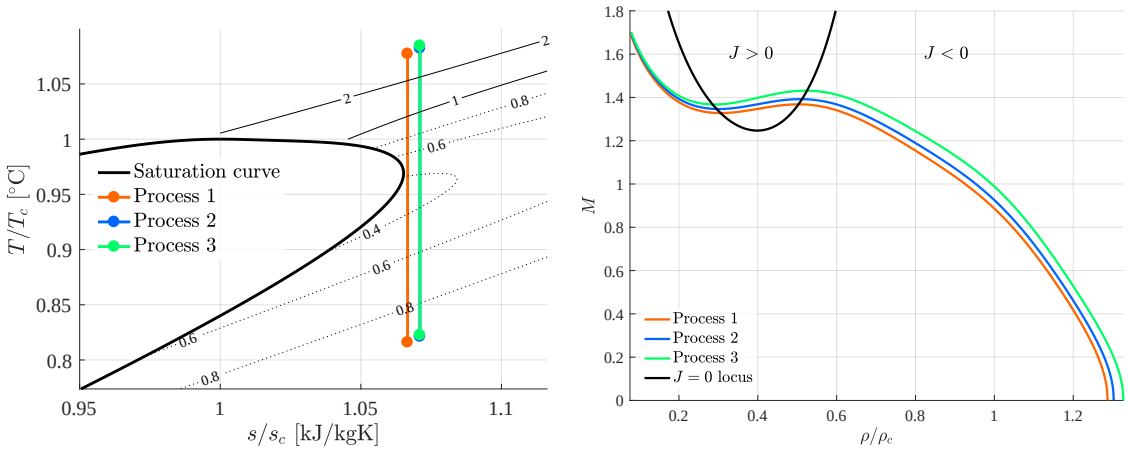

(a) (b)

Figure 1: (a) The three isentropic expansion processes reported on the temperature–entropy thermodynamic plane. Iso-Γ lines (dotted) are reported. (b) $M(\rho)$ locus. Reports the Mach number profiles for the three different processes.

In the ideal-gas case ($\Gamma > 1$), M is a monotone decreasing function of density ($J < 0$). For non-ideal flows ($\Gamma < 1$), three different cases can be distinguished, according to the sign of J. If $J < 0$ ($J > 0$), the Mach number is a decreasing (increasing) function of density. The states matching the condition $J = 0$ are stationary points of the $M(\rho)$ function and for these states the following relation holds:

$$M(\rho; \bar{s}, \bar{h}^t)_{J=0} = \sqrt{\frac{1}{1 - \Gamma(\rho; \bar{s}, \bar{h}^t)}} \tag{5}$$

For the non-ideal classical regime of interest in the present work ($0 < \Gamma < 1$), the Mach number given by eq. 5 is always greater than 1, thus the Mach number can attain a non-monotone profile only in the supersonic portion of the nozzle. Remarkably, the $M(\rho)$ function explicitly depends on the value of the fundamental derivative of gasdynamics Γ, which in turn embeds the dependence on reservoir conditions. In the nozzle design phase, the Mach number profile along the expansion can thus be shaped by adjusting the thermodynamic state of the fluid at the inlet.

The temperature–entropy thermodynamic plane of Fig. 1(a) reports the liquid-vapor

saturation curve of MM and selected isolines of the fundamental derivative of gasdynamics Γ. On the diagram, three isentropic supersonic expansions, characterized by a non-monotone Mach profile, are indicated. Operating conditions are reported in Tab. 1. Reservoir states are located above the critical point of MM ($T_c = 245.55$℃, $P_c = 19.394$ bar), while the thermodynamic conditions at nozzle exhaust belong to the single-phase vapor region, below the critical point. The corresponding Mach profiles (cf. eq. 2) are reported in Fig. 1(b). Thermodynamic properties are computed using the Span-Wagner (SW) multiparameter Equation of State (EoS) [9], a state-of-the-art thermodynamic model accounting for non-ideal flow behaviour.

In order to obtain meaningful measures of pressure, temperature and Mach number, it is fundamental to realize an expansion in the single-phase vapor region only. Moreover, in order to avoid significant structural decomposition of MM vapor during operation, the reservoir thermodynamic state must be set below the thermal stability limit of the fluid. Recently (see Ref. [7]), the thermal stability of MM was studied in a dedicated experimental facility and the onset of fluid thermal decomposition was observed at a temperature of 240℃. Nevertheless, according to experimental results reported in Ref. [8], ORC plants can be safely operated with MM up to a heat source temperature of 300℃. In state-of-the-art ORC plants, the maximum operating temperature is about 290℃, while the standard temperature range in which the evaporation process is carried out is 180-250℃, as documented in Ref. [15]. The operating conditions reported in Tab. 1 are suitable for the observation of nozzle expansions featuring a non-monotone Mach profile in the single-phase vapor region of MM, while still operating the test rig below the thermal stability limit of the working fluid.

2.3 Nozzle design

Gasdynamic nozzles operating in the NICFD regime are designed for a particular working fluid, exhaust Mach number and reservoir thermodynamic state, due to the dependence of the expansion process on the fundamental derivative of gasdynamics. The unsteady operation of the TROVA wind tunnel is such that the total thermodynamic state attained in the settling chamber changes continuously during the test, due to the emptying of the HPV. As a consequence, the nozzle works mostly in off-design conditions.

With this in mind, a set of nozzles suitable for the observation of the non-monotone Mach profile in the TROVA wind tunnel are considered. The supersonic portion of the nozzle is designed using the *Method of Characteristics* (MOC) implemented in Ref. [6], which includes state-of-the-art EoS. In the present work, the design process is performed using the Span-Wagner EoS. Input parameters to the MOC are the reservoir state (P^t, T^t) and the exhaust pressure P_e. The latter is computed with the quasi-one-dimensional approach and the SW EoS to obtain an exhaust Mach number $M_e = 1.7$. Once the non-dimensional geometry of the diverging portion of the nozzle is determined from MOC design, an appropriate scaling of the geometry based on the throat half-height H is performed and the converging portion is designed. Due to the batch operating mode of the TROVA, the thermodynamic conditions in which the non-monotone Mach profile is observable can be attained only at test start. An increase in the testing time, which can be obtained by re-

	Design point			*Uncertainties*		*Geometrical parameters*	
Nozzle	P^t [bar]	T^t [°C]	P_e [bar]	U_{P_T} [bar]	U_{T_T} [°C]	H	R_t
N1	29	264.53	4.81	0.028	0.189410	8.5 mm	$30H$
N2	30	265.76	4.93	0.028	0.786506	7.2 mm	$40H$
N3	31	266.35	5.03	0.028	0.803919	12.5 mm	$5H$
N4	31	266.35	5.03	0.028	0.793639	7.3 mm	$40H$

Table 2: Design operating conditions and geometrical parameters for nozzles $N1$, $N2$, $N3$, and $N4$ of Fig. 2 (a), (c), (e), (g)

ducing the mass-flow rate discharged by the nozzle (i.e. by reducing H), is thus desirable, since it would allow to extend the time interval in which the non-monotone variation of the Mach number can be observed. In the experiments, the occurrence of a non-monotone Mach number profile along the nozzle axis can be assessed from schlieren images, which provide a direct measurement of the flow Mach number (see Sec. 2.1). In case schlieren images are not available, the Mach number can be computed a-posteriori starting from the total thermodynamic state, as measured in the settling chamber, and from the static pressures, measured along the test section. The number of measurement points in the non-monotone region of the Mach number profile is conditioned by the finite dimension of the sensors. Their number can be raised by either enlarging the throat half-height H or by increasing the radius of curvature of the nozzle profile R_t at the throat.

Figures 2 (a), (c), (e), and (g) report four possible geometrical layouts of the TROVA test section. For each nozzle, labeled $N1$, $N2$, $N3$, and $N4$, Tab. 2 provides the design operating conditions and the geometrical parameters. The design points for nozzles $N1$ and $N2$ correspond to *Process 1* and *Process 2* of Tab. 1, respectively, while *Process 3* of Tab. 1 is the design point for both nozzles $N3$ and $N4$. For each nozzle profile reported in Fig. 2 (a), (c), (e), (g), three different branches are distinguished. The dashed lines identify the converging portions, which are defined by 5^{th}-order polynomial curves matched smoothly with a circular arc of radius R_t at the throat. The so-called *expansion region* of the nozzle, i.e. the region in which expansion to the desired Mach number is performed, is represented with a solid line. This branch of the nozzle profile is located immediately downstream of the throat, and it is defined by a circular arc of radius R_t. The dotted line identifies the so-called *turning region* of the nozzle, which is devoted to the generation of a parallel uniform flow at nozzle exhaust. The plot also reports the optically accessible region of the test section (gray box) and the position of pressure measurement points along the nozzle axis (black dots). For each nozzle, Fig. 2 (b), (d), (f), and (h) report the pressure and Mach number profiles along the nozzle axis, as resulting from nominal conditions. The plots are limited to the diverging portion of the nozzle, where the solution of the flow-field computed with the Method of Characteristics is available.

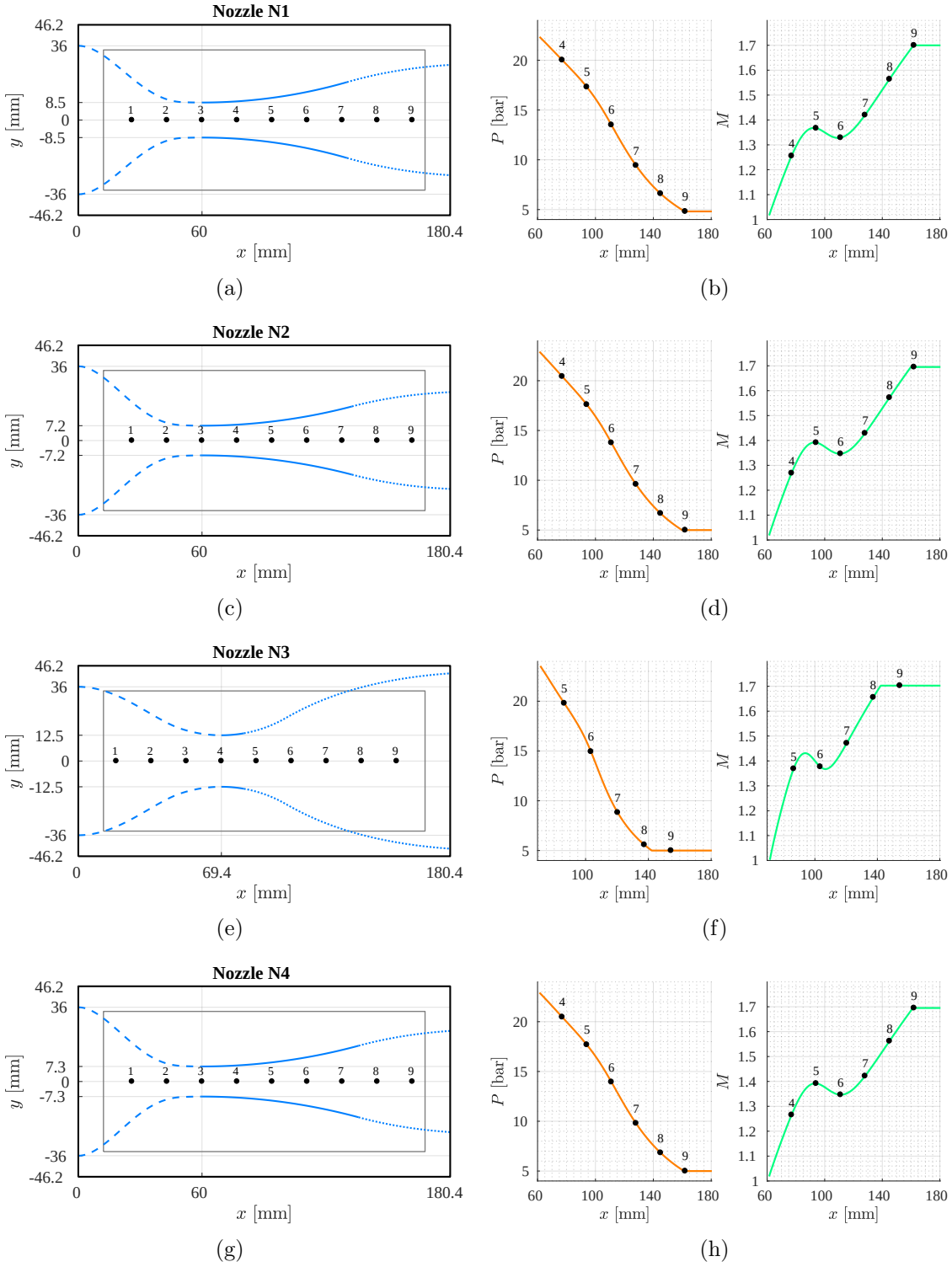

Figure 2: (a), (c), (e), (g) Geometrical layout of the TROVA test section for four different nozzle designs. (b), (d), (f), (h) Pressure P and Mach number M profiles along the symmetry axis of the diverging portion resulting from the MoC solution of the supersonic flow-field, complemented with the SW EoS.

3 UNCERTAINTY QUANTIFICATION FRAMEWORK

The design procedure was enrolled without taking into account the fact that the nominal design conditions are not exactly reproducible in the actual test rig. The not perfect control over the state of the fluid at the inlet of the test section thus translates into uncertainty on the actual operating conditions. Therefore, the nozzle could work outside its design regime and the expected non-monotonic Mach trend could not occur. Consequently, it is of utmost importance to assess the behavior of the nozzle under uncertain over the operating conditions. Since the TROVA is a blow down facility, the initial pressure in the HPV must be set to a value higher than the design one. As the discharge is continuous, there will necessarily be a given time instance in which the total pressure in the settling chamber match exactly the desired value. Concerning the total pressure, we can therefore assume that the uncertainty is related to our the accuracy of our knowledge, which of course is defined by measurements. On the other hand, it is nearly impossible that in the very same instance the total temperature will match its design value as well. For temperature, it follows that we can not just limit the the uncertainty to measurements. On the other hand, all the processes are occurring in the close proximity of the saturation curve, so it is reasonable to consider that the worst case scenario would be to enter the two-phase region.

Forward Uncertainty Quantification methods allow to propagate the uncertainties over inputs to a Quantity of Interest (QoI). In our case, the goal of forward propagation is then to assess the variability of the Mach number. To enroll this analysis, a non-intrusive Polynomial Chaos Expansion (PCE) approach (see [3]) is exploited.

In a non-intrusive PCE approach, the mathematical model through which the uncertainties have to be propagated is replaced by a spectral expansion. Following the original theory of Wiener on spectral representation of stochastic processes, the PCE may be written as:

$$u(\mathbf{x}, t, \boldsymbol{\xi}) = \sum_{\alpha} u_\alpha(\mathbf{x}, t)\Psi_\alpha(\boldsymbol{\xi}), \tag{6}$$

The vector $\boldsymbol{\xi}$ gathers a set of independent random variables $\xi_i, i = 1, 2, \cdots, n_\xi$. One should bear in mind that α are multi-indexes, $\alpha = (\alpha_1, \alpha_2, ..., \alpha_n)$ with each component $\alpha_i = (0, 1, ...)$ while Ψ_α are multivariate polynomial functions, orthogonal with respect to the probability distribution function of the vector $\boldsymbol{\xi}$. The terms $u_\alpha(x, t)$ are the so-called PCE coefficients. In general, the PCE includes an infinite number of polynomials but, in practice, the PCE is truncated to a certain degree No ($|\alpha|_1 \leq$ No) To compute the PCE coefficients, a quadrature formulae was employed (see [3] for details). To this extent, one must first gather a certain number of realizations, i.e. a collection deterministic solutions obtained using different input parameters sampled from the stochastic space. This set is usually referred to as the Design of Experiment (DoE).

In this work, a Non Intrusive Spectral Projection method (NISP) (see Ref. [3]), was used to build the PCE. Once the surrogate model is built, it is straightforward to compute

the mean (E) and variance (V) of the original random process $u(\mathbf{x}, t)$ as:

$$E(u(\mathbf{x},t)) = u_0(\mathbf{x},t), \quad V(u(\mathbf{x},t)) = \sum_\alpha u_\alpha^2(\mathbf{x},t). \tag{7}$$

4 RESULTS

This section presents the assessment of the expected expansion processes under the considered uncertainties, for N1, N2, N3 and N4.

As pointed out in Sec. 3, we take into account the uncertainties over the values of total pressure and total temperature of the fluid at the inlet of the test section. Regarding the total pressure, the uncertainty is given by the measurements chain: a uniform distribution $P_0 \sim \mathcal{U}(P_{meas} - \delta, P_{meas} + \delta)$, with P_{meas} being the measured value and $\delta \approx 0.07\%$ of the probe end scale value. The maximum admissible total temperature bias is instead computed using the FluidProp library [2] and, in the following, the value is again assumed to be uniformly distributed within the computed range. Tab. 2 reports the considered uncertainty for each nozzle.

The nozzle N1 is immediately discarded as the expansion takes place too close to the liquid-vapor saturation curve and the margin over the temperature is too limited ($\delta = 0.189410$ [℃]). The most limiting variation, $\delta = 0.786506$ [℃], is therefore considered among all the other experiments.

To generate the DoE, a polynomial up to the 3rd order was considered, therefore each DoE resulted in a set of 16 realizations.

Each realization was enrolled using the Non-Ideal CFD solver included in the SU2 open-source suite [4, 5] and exploiting the Peng-Robinson EoS included in the embedded thermodynamic library. A grid sensitivity analysis was first carried out, to choose a grid with an appropriate spatial resolution. All the simulation were enrolled using a second-order scheme and under the assumption of a non-viscous flow. This latter hypothesis is justified by the fact that the QoI is measured at the nozzle centerline, a region which is mostly governed by non viscous dynamics. Moreover, the smoothness of the geometry helps keeping the boundary layer over walls to a limited thickness.

Once the realization were enrolled, the PCE was built and exploited to extract the statistics of the QoI. Results shown that the convergence of the stochastic quantities is reached by considering a 2nd order polynomials

Fig. 3(a) reports the mean pressure trend along the axis of each nozzle. In Fig. 3(b), the standard deviation depending on the x coordinate is plotted. The three nozzles are similarly affected by the considered uncertainty: the trend is qualitative equal and just small differences are noticeable in terms of maximum deviation. Nevertheless, $N4$ shows the most limited deviation in the supersonic region, i.e. where the Mach number can possibly attain a non-monotone profile. Fig. 3(c) and 3(d) reports the mean and the standard deviation related to the Mach number: the non-monotonic non-ideal variation is confirmed. In particular, $N2$ and $N4$ show a smooth trend while $N3$ is characterized by steeper gradients. The standard deviation plot reveals that nozzle $N2$ is the one that suffers the less, though the difference is yet not so relevant, from the considered uncertainties.

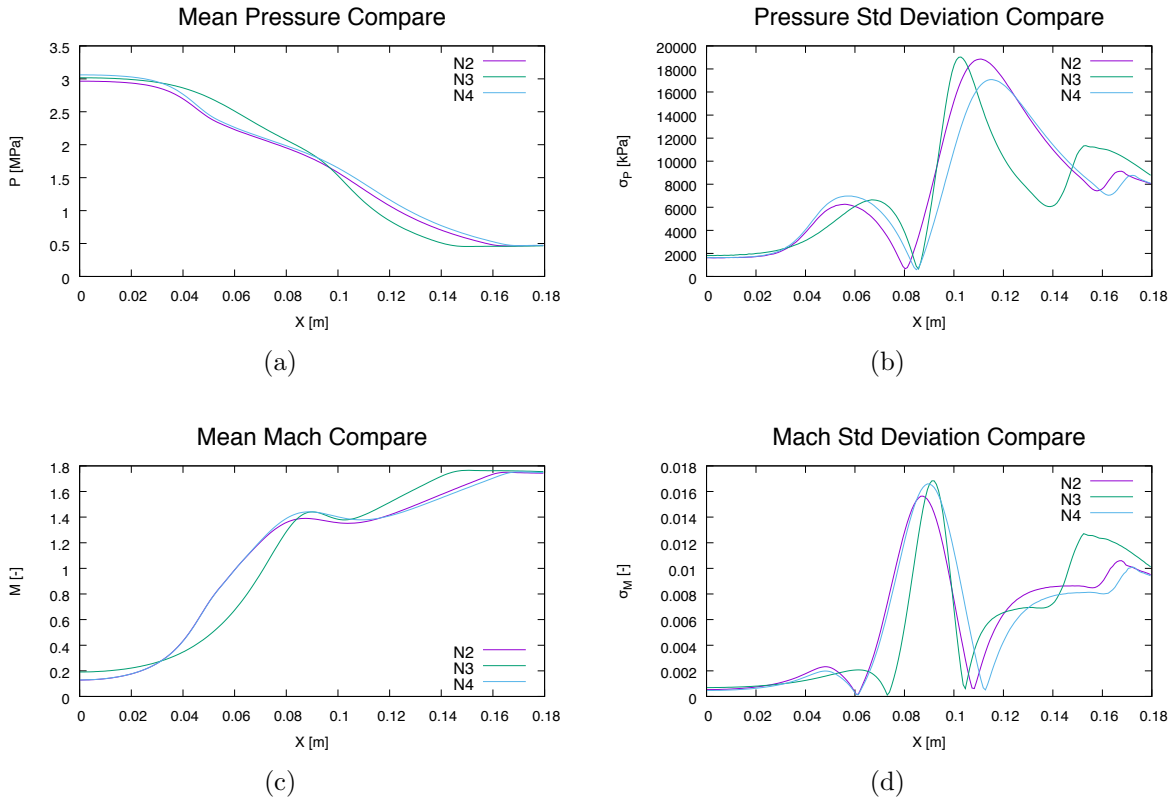

Figure 3: Mean trend (static pressure (a) and Mach number (c)) and related standard deviation (static pressure (b) and Mach number (d)), along the nozzle centerline.

In Fig. 4 the Mach envelope is plotted, i.e. the bounds identified by the curves $\mu_M + \sigma_M$ and $\mu_M - \sigma_M$ (where μ_M is the mean value and σ_M the standard deviation).

The picture reveals that the non-monotonic behavior is obtained even for the worst case $\mu_M - \sigma_M$, for each nozzle. Nevertheless, between the considered set $N2$ has the smallest difference between the local maximum and the local minimum ($\Delta \approx 3.8\dot{1}0^{-2}$ in the worst case scenario) while $N3$ and $N4$ show a similar behavior ($\Delta \approx 6.24\dot{1}0^{-2}$).

5 CONCLUSIONS

This work presents the design procedure of a converging-diverging nozzle addressed to reproduce a supersonic non-ideal expansion of a MM siloxane flow. In particular, the goal was to obtain a non-ideal non-monotonic Mach number variation through the expansion. Four different experiments were designed. Each experiment includes a specific nozzle geometry and operating conditions. The role of uncertainties affecting the operating condition over the flow configuration within the test section were assessed by exploiting a Forward Uncertainty propagation technique. The reported analysis shows how the uncertainties propagates through the model and allow to assess the robustness of each

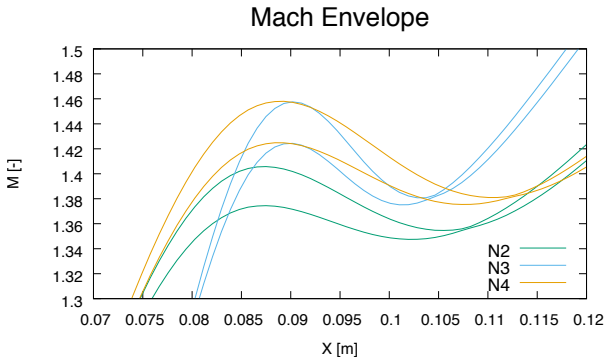

Figure 4: Mach number σ envelope ($\mu \pm \sigma$)

experiment. The nozzle referred to a $N4$ is characterized by the largest difference between the local maximum and minimum of the non-monotonic Mach number trend and the most limited pressure deviation with respect of the considered uncertainties. The smoothness of the gradients in the Mach number curve results in a desirable increase of the spatial range in which the non-monotone distribution is attained. Based on this analysis, the nozzle $N4$ is identified as the most promising candidate to be employed in the actual experiment.

ACKNOWLEDGEMENTS

The authors would like to thanks Andrea Spinelli for the fruitful discussions that fostered the development of this work. This work is partially funded by the European Commission's H2020 program, through the UTOPIAE Marie Curie Innovative Training Network, H2020-MSCA-ITN-2016, Grant Agreement number 722734 and by the European Research Council under Grant ERC Consolidator 2013, project NSHOCK 617603.

REFERENCES

[1] P. Colonna, E. Casati, C. Trapp, T. Mathijssen, J. Larjola, T. Turunen-Saaresti, and A. Uusitalo. Organic Rankine Cycle Power Systems: From the Concept to Current Technology, Applications and an Outlook to the Future. *ASME Journal of Engineering for Gas Turbines and Power*, 137:100801, 2015.

[2] P Colonna and TP Van der Stelt. Fluidprop: a program for the estimation of thermo physical properties of fluids. *Energy Technology Section, Delft University of Technology, Delft, The Netherlands, http://www. FluidProp. com*, 2004.

[3] T. Crestaux, O. Le Maître, and J-M. Martinez. Polynomial chaos expansion for sensitivity analysis. *Reliability Engineering & System Safety*, 94(7):1161–1172, 2009.

[4] Thomas D. Economon, Dheevatsa Mudigere, Gaurav Bansal, Alexander Heinecke, Francisco Palacios, Jongsoo Park, Mikhail Smelyanskiy, Juan J. Alonso, and Pradeep

Dubey. Performance optimizations for scalable implicit {RANS} calculations with {SU2}. *Computers & Fluids*, 129:146 – 158, 2016.

[5] G. Gori, M. Zocca, G. Cammi, A. Spinelli, and A. Guardone. Experimental assessment of the open-source su2 cfd suite for orc applications. *Energy Procedia*, 129(Supplement C):256 – 263, 2017.

[6] A. Guardone, A. Spinelli, and V. Dossena. Influence of Molecular Complexity on Nozzle Design for an Organic Vapor Wind Tunnel. *ASME Journal of Engineering for Gas Turbines and Power*, 135:042307, 2013.

[7] L. Keulen, C. Landolina, A. Spinelli, P. Iora, C. Invernizzi, L. Lietti, and A. Guardone. Design and commissioning of a thermal stability test-rig for mixtures as working fluids for orc applications. *Energy Procedia*, 129:176 – 183, 2017.

[8] Markus Preiinger and Dieter Brggemann. Thermal stability of hexamethyldisiloxane (mm) for high-temperature organic rankine cycle (orc). *Energies*, 9(3), 2016.

[9] R. Span and W. Wagner. Equations of State for Technical Applications. I. Simultaneously Optimized Functional Forms for Nonpolar and Polar Fluids. *Int. J. Thermophys.*, 24(1):1–39, January 2003.

[10] A. Spinelli, G. Cammi, M. Zocca, S. Gallarini, F. Cozzi, V. Dossena, P. Gaetani, and A. Guardone. Experimental observation of supersonic non-ideal compressible-fluid nozzle flows of siloxane MDM. *Energy Procedia*, 129(Supplement C):1125–1132, 2017.

[11] A. Spinelli, F. Cozzi, G. Cammi, M. Zocca, P. Gaetani, V. Dossena, and A. Guardone. Preliminary characterization of an expanding flow of siloxane vapor MDM. *Journal of Physics: Conference Series*, 821(1):012022, 2017.

[12] A. Spinelli, M. Pini, V. Dossena, P. Gaetani, and F. Casella. Design, Simulation, and Construction of a Test Rig for Organic Vapours. *ASME Journal of Engineering for Gas Turbines and Power*, 135:042303, 2013.

[13] P. A. Thompson. A Fundamental Derivative in Gasdynamics. *Physics of Fluids*, 14(9):1843–1849, 1971.

[14] P. A. Thompson. *Compressilbe-Fluid Dynamics*. McGraw-Hill, 1988.

[15] Riccardo Vescovo and Emma Spagnoli. High temperature orc systems. *Energy Procedia*, 129:82 – 89, 2017.